Proceedings of the 2008 International Design Engineering Technical Conference & Computers and Information and Information in Engineering Conference
IDETC/CIE 2008
August 3-6, 2008, New York City, NY, USA

DRAFT

DETC2008-49062

DYNAMIC OBSERVER METHOD BASED ON MODIFIED GREEN'S FUNCTIONS FOR ROBUST AND MORE STABLE INVERSE ALGORITHMS

Priscila F. B. Sousa
Federal University of Uberlândia-School of Mechanical Engineering, Brazil

Ana P. Fernandes
Federal University of Uberlândia-School of Mechanical Engineering, Brazil

Valério Luis Borges
Federal University of Uberlândia-School of Mechanical Engineering

George S. Dulikravich
Florida International University- Department of Mechanical and Materials Eng., Miami, FL, USA

Gilmar Guimarães
Federal University of Uberlândia-School of Mechanical Engineering, Brazil

ABSTRACT

This work presents a modified procedure to use the concept of dynamic observers based on Green's functions to solve inverse problems. The original method can be divided in two distinct steps: i) obtaining a transfer function model G_H and; ii) obtaining heat transfer functions G_Q and G_N and building an identification algorithm. The transfer function model, G_H, is obtained from the equivalent dynamic systems theory using Green's functions. The modification presented here proposes two different improvements in the original technique: i) A different method of obtaining the transfer function model, G_H, using analytical functions instead of numerical procedures, and ii) Definition of a new concept of G_H to allow the use of more than one response temperature. Obtaining the heat transfer functions represents an important role in the observer method and is crucial to allow the technique to be directly applied to two or three-dimensional heat conduction problems. The idea of defining the new G_H function is to improve the robustness and stability of the algorithm. A new dynamic equivalent system for the thermal model is then defined in order to allow the use of two or more temperature measurements. Heat transfer function, G_H can be obtained numerically or analytically using Green's function method. The great advantage of deriving G_H analytically is to simplify the procedure and minimize the estimative errors.

INTRODUCTION

The inverse problem can be found in a large area of science and engineering and can be applied in different ways. The great advantage of this technique is the ability of obtaining the solution of a physical problem that can not be solved directly.

Different techniques can be found in literature in the solution of inverse heat conduction problem (IHCP). For instance, the mollification method [1], the conjugate gradient technique [2], the sequential function specification [3] or the use of optimization techniques such as genetic algorithms [4], simulated annealing [5] or golden section method [6]. Technique based on filter such as the Kalmn filter [7] or dynamic observers [8,9] have also been employed for the solution of the IHCP.

In the dynamic observer technique, the IHCP solution algorithms are interpreted as filters passing low-frequency components of the true boundary heat flux signal while rejecting high-frequency components in order to avoid excessive amplification of measurement noise [8]. The dynamic observers technique proposed by Blum and Marquardt [8], focused on the one-dimensional linear case, was extended to solve an inverse multidimensional heat conduction problem by Sousa et al. [9].

In order to deal with multidimensional thermal models, Sousa proposed an alternative way of obtaining the heat transfer function, G_H, by using the Green function concept instead of taking the Laplace transform of the spatially discretized system. This procedure allows flexibility and efficiency to solve multidimensional inverse problems.

Despite the flexibility and efficiency of this procedure the way proposed in ref. [9] is complex and requires some ability to obtain the heat transfer function. In order to simplify the procedure, minimize the noise effect in G_H, and give more robustness and stability to the inverse algorithms some modifications are proposed here.

This work proposes two different improvements in the original technique: i) A different method of obtaining the transfer function model, G_H, using analytical functions instead of numerical procedure, and ii) Definition of a new concept of G_H to allow the use of more than one temperature response.

NOMENCLATURE

a, b, c, L	plate dimensions, m
k	thermal conductivity, W/m^2 K
q	heat flux input, W/m^2
T	temperature, ^{o}C
t	time, s
T_0	initial temperature
x, y, z	Cartesian coordinates, m
Y	measured temperature, ^{o}C
f	frequency, Hz
G	Green's function, m^{2}K/W
G_H	heat conductor transfer function, m^{2}K/W
G_Q	signal transfer function, m^{2}K/W
G_N	noise transfer function, m^{2}K/W
s	Laplace transform variable
X(*t*)	input signal in time domain, W/m^2
Y(*t*)	output signal in time domain, ^{o}C
X(*f*)	input signal in frequency domain, W/m^2

Greek Symbols

α	thermal diffusivity, m^2/s
ρ	density, kg/m^3
θ	temperature difference, ^{o}C

Subscripts

M	relative to experimental data
i	relative to integer variables

FUNDAMENTALS

The inverse problem solution based on dynamic observers can be divided in two distinct steps: i) the obtaining of the transfer function model G_H; ii) the obtaining of the heat transfer functions G_Q and G_N and the building algorithm identification. A complete description of this technique can be found in the work of Blum and Marquardt [8] and Sousa et al. [9].

This section presents a new procedure based on analytical Green function concept to obtain the transfer function model.

Thermal problem

Figure 4 presents a 2D-transient thermal problem that can be described by diffusion equation as

$$\frac{\partial^2 \theta}{\partial x^2} + \frac{\partial^2 \theta}{\partial y^2} = \frac{1}{\alpha}\frac{\partial \theta}{\partial t} \tag{1a}$$

In the region R (0 < x < L, 0 < y < W) and t> 0, subjected to the boundary condition

$$\begin{aligned} -k\left.\frac{\partial \theta}{\partial x}\right|_{x=0} &= q(t) \quad on\ S_1\ (0 \le y \le y_h) \\ -k\left.\frac{\partial \theta}{\partial x}\right|_{x=0} &= 0 \quad on\ S_2\ (y \ge y_h) \end{aligned} \tag{1b}$$

$$\left.\frac{\partial \theta}{\partial y}\right|_{y=0} = \left.\frac{\partial \theta}{\partial y}\right|_{y=W} = \left.\frac{\partial \theta}{\partial x}\right|_{x=L} = 0 \tag{1c}$$

and initial condition

$$\theta(x, y, z, 0) = T(x, y, t) - T_0 \tag{1d}$$

where y_H is the boundary where the heat flux is applied.

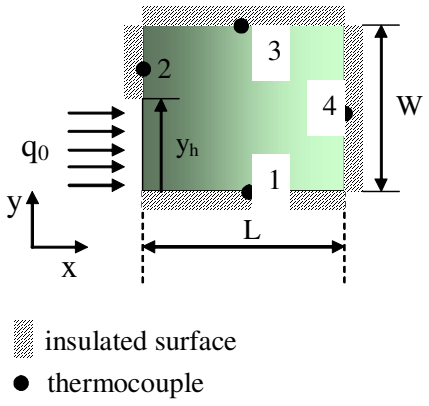

Figure 1. Thermal problem

The solution of Eqs. (1) can be given in terms of Green's function as in [10].

$$\theta(x, y, t) = \int_{\tau=0}^{t} \left[G_H(x, y, t-\tau)\ q(\tau) \right] d\tau \tag{2}$$

where

$$G_H(x, y, t-\tau) = \frac{\alpha}{k}\int_0^{y_h} G_H^+(x, y, t-\tau / x', y')\Big|_{x'=0} dy' \tag{3}$$

and $G_H^+(x, y, t-\tau)$ represents the Green function of the thermal problem given by Eqs.(1).

Equation (2) reveals that an equivalent thermal model can be associated with a dynamic model. It means, a response of the input/output system can be associated to Eq.(2) in the Laplace domain as the convolution product

$$\theta(x, y, t) = G_H(x, y, t-\tau) * q(\tau) \tag{4}$$

This dynamic system can be represented as shown in Fig. (2).

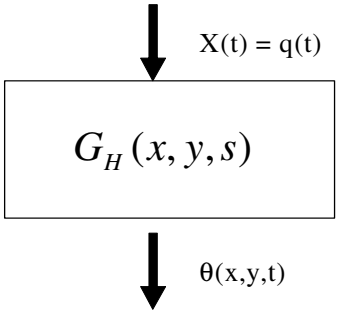

Figure 2. Dynamic thermal model system

Equation (4) can also be evaluated in the Laplace domain as a single product [11]

$$\bar{\theta}(\mathrm{x}, y, z, s) = \bar{G}_H(x, y, s)\ \bar{q}(s) \tag{5}$$

where the Laplace transform of a *F(t)* function is defined by

$$L[F(t)] = \bar{F}(s) = \int_t^{\infty} e^{-st'} F(t')\, dt' . \tag{6}$$

If heat transfer function, $\bar{G}_H(x, y, s)$, and temperatures response $\bar{\theta}(\mathrm{x}, y, z, s)$ are available, Eq.(5) can be used in an inverse procedure to estimate the heat flux input, $\bar{q}(s)$. One way to estimate this heat flux input is to apply the dynamic observer technique [8,9] that will be described in the next section.

Dynamic observers technique

In order to estimate the input q the dynamic system given by Eq.(5) can also be represented by a block diagram shown in Fig. 3.

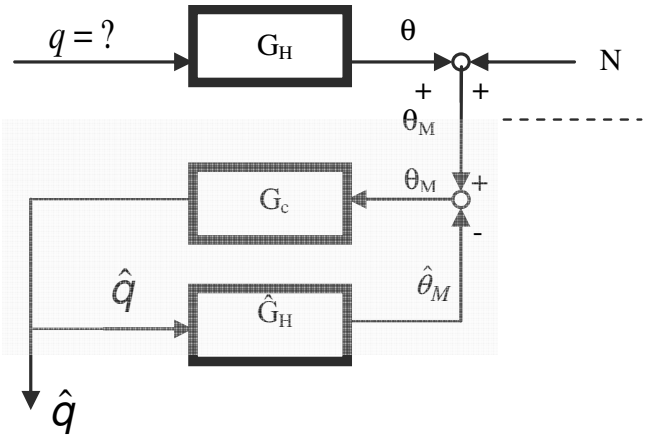

Figure 3. Frequency-domain block diagram [8]

It can be observed from the block diagram that:

i) the unknown heat flux ***q(s)*** is applied to the conductor (reference model), G_H, and results in a measurement signal θ_M corrupted by noise *N*,

$$\theta_M = \theta + N = G_H\ q + N \tag{7}$$

ii) The estimate value $\hat{q}$ is computed from the output data θ_M. Thus, the estimator can be represented in a closed-loop transfer function of the feedback loop (Fig. 3) as

$$\hat{q} = \frac{G_C}{1 + G_C G_H}\theta_M \tag{8}$$

that characterizes the behavior of the solution algorithm.

Substituting Eq.(7) in Eq.(8) we obtain

$$\hat{q} = \frac{G_C G_H}{1 + G_c G_H} q + \frac{G_C}{1 + G_c G_H} N \tag{9}$$

or

$$\hat{q} = G_Q\, q + G_N\, N \tag{10}$$

where $G_Q = \dfrac{G_C G_H}{1 + G_c G_H}$ and $G_N = \dfrac{G_Q}{G_H} = \dfrac{G_C}{1 + G_c G_H}$ (11)

The transfer function G_Q is chosen to have the behavior of type I chebychev filter and its frequency response magnitude assume the form

$$G_Q(s) = \frac{k_{cheb}}{(s - s_{Cheb,1})(s - s_{Cheb,2}) \cdots (s - s_{Cheb,n_Q})} \tag{12}$$

and G_N is identified by Eq.(11) provided that G_H is obtained.

Thus, from Eq. (8) the resulting algorithm can then be given by

$$\hat{q}(s) = G_N(s) \times \theta_M(s) \tag{13}$$

or in domain frequency

$$\hat{q}(jw) = G_N(jw) \times \theta_M(jw) \tag{14}$$

It can be observed in Eq. (10) that if the algorithm estimates the heat flux correctly, G_Q is equal to unity, $G_Q = 1$, and the frequency $\boldsymbol{w}$ is within the pass band. In this case, the noise transfer function G_N is equal to the inverse transfer function of the heat conductor (G_H^{-1}).

According to Blum and Marquardt [8] the observer is essentially an on-line scheme. In this case, estimation of the heat flux at the current time step is based on current and past temperature measurements only. In this case, any on-line estimator involves a phase shift or lag. To remove this lag Blum and Marquardt proposed a filtering procedure that can be resumed in the use of two discrete-time difference equations

$$q(k) = \sum_{i=0}^{n_n} b_i Y_M(k-i) - \sum_{i=1}^{n_n} a_i q(k-i) \tag{15}$$

and

$$\hat{q}(k) = \sum_{i=0}^{n_n} b_i q(k-i) - \sum_{i=1}^{n_n} a_i \hat{q}(k-i) \tag{16}$$

The coefficients $\boldsymbol{a_i}$ and $\boldsymbol{b_i}$ that appear in Eqs.(15) and (16) are obtained using Eq.(11). In this case, the inverse procedure is concluded with the $\overline{G}_H(x, y, s)$ identification.

Previous work presented by Sousa et al. [9] proposes the identification of $\overline{G}_H(x, y, s)$ based on the cross correlation of two functions of stationary random and in polynomial function adjust of a particular sampled interval. Although efficient, the technique requires some user's ability that adds some complexity to the optimization procedure.

The new procedure proposed here is to obtain the heat transfer $\overline{G}_H(x, y, s)$ in an exact and analytical way.

Analytical heat transfer function identification, G_H.

If the dynamic system is linear, invariant and physically invariable [11] the response function $\overline{G}_H(x, y, z, s)$ is the same, independently of the pairs input/output. In this case, the heat transfer function $\overline{G}_H(x, y, z, s)$ can, then, be obtained through the auxiliary problem that is a homogenous version of the original problem. The auxiliary problem is then solved for the same region with a zero initial temperature and unit impulsive source located at the region of the original heating here represented by $\overline{\theta}^+(\mathrm{x}, y, z, s)$.

It means $\overline{G}_H(x, y, z, s)$ can be obtained using Eq.(5) as

$$\overline{G}_H(x, y, z, s) = s \ \overline{\theta}^+(\mathrm{x}, y, z, s) \tag{17}$$

where s and $\overline{\theta}^+(\mathrm{x}, y, z, s)$ represent the Laplace transform of a unit constant, $L[1] = \frac{1}{s}$, and a Laplace transform of the temperature response of a unit step heat flux, $\theta^+(\mathrm{x}, y, t)$, respectively.

Temperature $\theta^+(\mathrm{x}, y, t)$ can then be obtained by using Green's function method to solve the thermal problem described by Eqs.(1) with heat flux input as

$$q = 1\ W/m^2 \ on\ S_1 \ (0 \le y \le y_h) \text{ and } q = 0 \ \ on\ S_2 \ (y \ge y_h) \tag{18}$$

Thus, the solution of the problem given by Eqs.(1) considering Eq.(18) is

$$\theta^+(\mathrm{x}, y, t) = \ + \frac{\alpha}{k} \int_{y'}^{y_H} \int_{\tau=0}^{t} G_{xy}(\mathrm{x}, y, t/x', y', t-\tau) \ \Big|_{x'=0} d\tau dy' \tag{19}$$

where

$$G_{xy}(\mathrm{x}, y, t/x', y', \tau) = G_x(\mathrm{x}, t/x', \tau) G_y(y, t/y', \tau) \tag{20}$$

As the homogenous condition in both direction x and y are the same, the Green functions can be given by

$$G_x = \frac{1}{L} + \sum_{m=1}^{\infty} \frac{e^{-A_m t} \cos(\beta_m x/L) \cos(\beta_m x'/L)}{N_1} \tag{21}$$

$$G_y = \frac{1}{W} + \sum_{m=1}^{\infty} \frac{e^{-A_m t} \cos(\gamma_n y/W) \cos(\gamma_n x'/W)}{N_2} \tag{22}$$

where $\frac{1}{N_1} = \frac{2}{L}, \frac{1}{N_2} = \frac{2}{W}, \beta_m = m\pi, \gamma_n = n\pi$

$$A_m = \left(\frac{\beta_m}{L}\right)^2 \alpha \text{ and } B_n = \left(\frac{\gamma_n}{W}\right)^2$$

The substitution of Eqs.(20-22) into Eq.(19) gives

$$\theta^+(\mathrm{x}, y, t) = \left[\sum_{n=1}^{\infty} Ax_m + \sum_{m=1}^{\infty} Ay_n + \sum_{n=1}^{\infty} Axy_{mn} \right] + A_1 t - \left[\sum_{m=1}^{\infty} Ax_m e^{-A_m t} + \sum_{n=1}^{\infty} Ay_n e^{-B_n t} + \sum_{n=1}^{\infty} \sum_{m=1}^{\infty} Axy_{mn} e^{-F_n t} \right] \tag{23}$$

where

$$F_n = (A_n + B_n) = \left(\frac{\beta_n^{*\,2}}{L^2} + \frac{\gamma_n^{*\,2}}{W^2} \right) \alpha \text{ and}$$

$$A_1 = +\alpha \frac{1}{k} \frac{W_1}{WL}$$

$$Ay_n = +\alpha \frac{1}{kL} \cos(\gamma_n^* y / W)\ W \frac{\sin(\gamma_n^* W_1 / W)}{N_2(\gamma_n^*)\gamma_n^*} \frac{1}{B_n}$$

$$Ax_m = \frac{1}{kW} W_1 W^2 \sum_{m=1}^{\infty} \frac{\cos(\beta_m^* x / L)}{N_1(\beta_m^*)} \frac{1}{A_m}$$

$$Axy_{mn} = \frac{\alpha}{k} \left[\frac{\cos(\beta_m^* x / L)}{N_1} \frac{\cos(\gamma_n^* y / W)}{N_2} \right] W \frac{\sin(\gamma_n^* W_1 / W)}{\gamma_n^*} \frac{1}{F_n}$$

Taking the Laplace transform of Eq.(23) we obtain

$$\bar{\theta}^+(\mathrm{x}, y, s) = \left[T_0 + \sum_{m=1}^{\infty} Ax_m + \sum_{n=1}^{\infty} Ay_n + \sum_{n=1}^{\infty} Axy_{mn} \right] \frac{1}{s} + A_1 \frac{1}{s^2} - \left[\sum_{m=1}^{\infty} Ax_m \frac{1}{s + A_m} + \sum_{n=1}^{\infty} Ay_n \frac{1}{s + B_n} + \sum_{n=1}^{\infty} \sum_{m=1}^{\infty} Axy_{mn} \frac{1}{s + F_{nm}} \right] \quad (24)$$

and therefore the heat transfer function in Laplace domains can be obtained by substituting Eq.(24) in Eq.(17) to give

$$\bar{G}_H(x, y, s) = s\, \bar{\theta}^+(\mathrm{x}, y, s) = \left[T_0 + \sum_{m=1}^{\infty} Ax_n + \sum_{n=1}^{\infty} Ay_m + \sum_{n=1}^{\infty} Axy_{mn} \right] + A_1 \frac{1}{s} - \left[\sum_{m=1}^{\infty} Ax_m \frac{s}{s + A_n} + \sum_{n=1}^{\infty} Ay_n \frac{s}{s + B_n} + \sum_{n=1}^{\infty} \sum_{m=1}^{\infty} Axy_{mn} \frac{s}{s + F_{nm}} \right] \quad (25)$$

Since Eq.(25) does not present any pole for s>0 then its inversion is stable. This fact guarantees more robustness to the inverse algorithm.

Multiple sensors

Estimators given by Eq.(15) and (16) were derived to be applied to single – input /output models. However, in order to minimize the noise that appears in measurement data it may be interesting to use more than one experimental measurement. In this case the use of Green's function method, with analytical or numerical approach, also allow with simplicity to generalize the use of that estimator. Following it will be formulated a dynamic system with two output points due to a single source. The extension for multiple points is very direct and immediate.

Figure 6 presents a single-input/two-output system. It means, this figure shows an equivalent dynamic system to a thermal problem given by Fig. 2 considering two thermocouples for different positions (1, 2). It is assumed here that noise terms $n_1(t)$ and $n_2(t)$ are uncorrelated with each other and with the input signal $q(t)$.

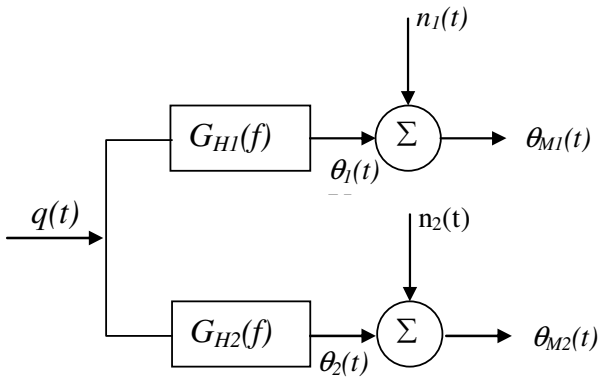

Figure 6. Single-input/two-output system.

In this case Eq.(4) gives

$$\theta(\mathrm{x_i}, y_j, t) = \int_{\tau=0}^{t} G_H(\mathrm{x_i}, y_j, t-\tau)\ q(\tau)\ d\tau \quad (26)$$

or in Laplace domain

$$\bar{\theta}(\mathrm{x}_1, y_1, s) = G_H(\mathrm{x}_1, y_1, s)\ q(s) \quad (27)$$

$$\bar{\theta}(\mathrm{x}_2, y_2, s) = G_H(\mathrm{x}_2, y_2, s)\ q(s) \quad (28)$$

Adding Eq.(27) to Eq.(28)

$$\bar{\theta}_1 + \bar{\theta}_2 = [G_{H1}(s) + G_{H2}(s)]\ q(s) \quad (29)$$

As Equation (29) has a similar representation of Eq.(5) the same estimators given by Eqs.(15) and (16) can be used to represent the single-input/two-output system. The only change that must be made is to consider the sum of temperature and the sum of heat transfer function in the system. As mentioned, the use of more than two thermocouples is immediate.

RESULTS AND DISCUSSION

This section presents two cases. First, the new procedure to obtain G_H is compared with the previous work [9] that also is based on Green function's principle but obtaining the heat transfer response using interval sample and numerical approach. The heat transfer function G_H is estimated from a two-dimensional transient problem that uses simulated data temperature measurements. Second, an experimental and controlled test is carried out.

Case 1 – Simulated case. Heat flux estimation using simulated data from only one position (one sensor).

The two-dimensional case described in Fig. (1) is analyzed in this section. Temperature distributions for the direct problem are generated using the solution of Eq. (1) considering a known

heat flux evolution q(t). Random errors are then added to these temperatures. The temperatures with error are then used in the inverse algorithm to reconstruct the imposed heat flux.

The simulated temperatures are calculated from the following equation

$$Y(L,t) = T(L,t) + \varepsilon_j \,. \tag{30}$$

where ε_j is a random number. The tests simulate an AISI 304 sample that is exposed to two different heat flux types respectively: i) a sinusoidal heat flux and; ii) a triangular heat flux. The parameter ε_j assumes values of 0, and within ± 5°C to sinusoidal and within ± 1°C to triangular heat flux. Both noises represent 5% of the maximum temperature for each heat fluxes. Figures 7 and 8 present the simulated temperature on position 1 shown in Fig. 2 and Table 1.

Figure 9 presents the modulus and phase of G_H obtained using Green function approach [9] and analytical method proposed here.

It can be observed that modulus and phase values are very close for values of frequencies less than 1 rad/s. Therefore, the difference in obtaining the value of G_H just depends on the cut frequency values. For this case, the cut frequency value chosen was w_c= 0.5rad/s.

Simulated data from four different positions are used to simulate one and more than one thermocouple. The positions, shown in Fig. 2 and denoted 1, 2, 3 and 4 are identified in Table 1. First, we will present estimation results by considering temperature simulated data using only one position (position 1). The use of more signals is discussed in the next section.

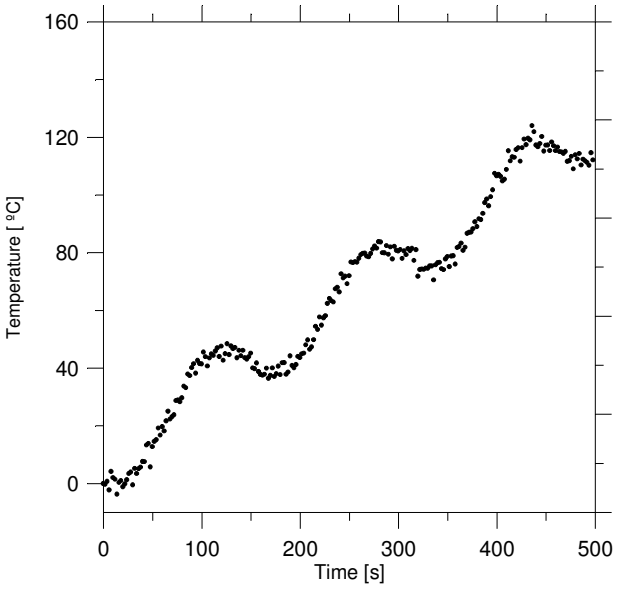

Figure 7. Experimental temperatures simulated numerically at x=0.05m and y=0.05m for a sinusoidal heat flux

Table 1. Geometry and simulated sensor position for Test 1

y_H=0.01m	L=0.01m	W=0.03 m
position	x_i 10^{-3}[m]	y_i10^{-3}[m]
1	5.0	0.0
2	0.0	15.0
3	10.0	15.0
4	5.0	30.0

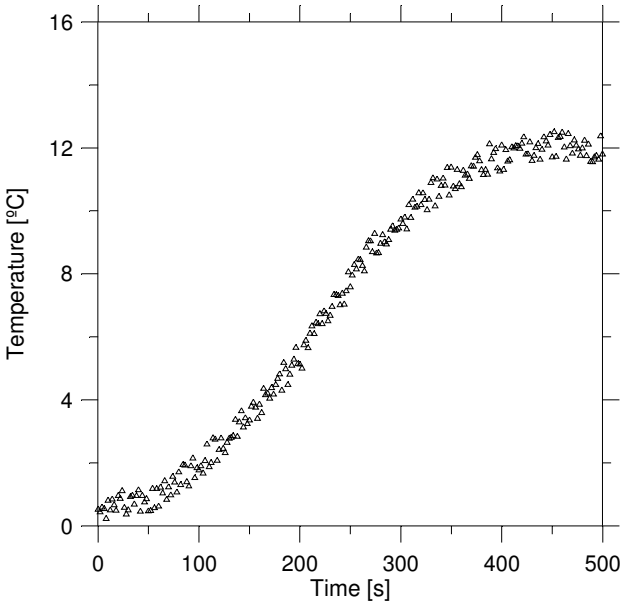

Figure 8. Experimental temperatures simulated numerically at x=0.05m and y=0.05m for a triangular heat flux

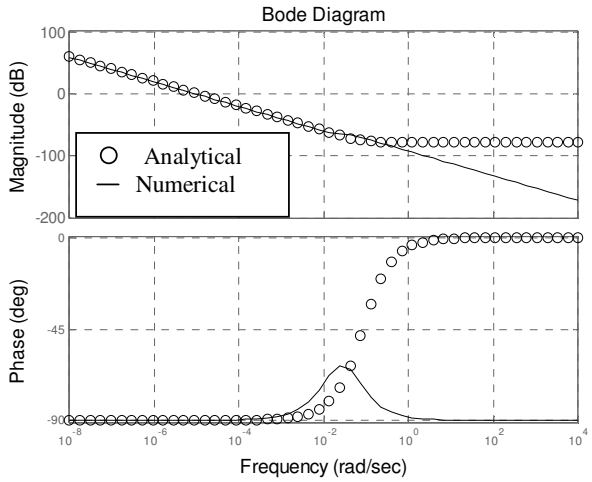

Figure 9. Modulus and phase of heat transfer function, G_H.

The heat flux estimates are shown in Figs. 10 and 11. These figures show the comparison between the heat flux estimated and the heat flux imposed for the two different kind of heat flux.

It can be observed that the results are also very closed. The great convenience in using the analytical form is the facility of obtaining the values for the position required while in numerical approach there are additional steps as adjusting or fitting data in interval samples. Besides that, the estimation is closer than numerical approach as can be observed in Fig. 10b and 11b that presents the difference among the two techniques with the heat flux imposed. For both heat fluxes the analytical G_H present better results in the heat flux estimation.

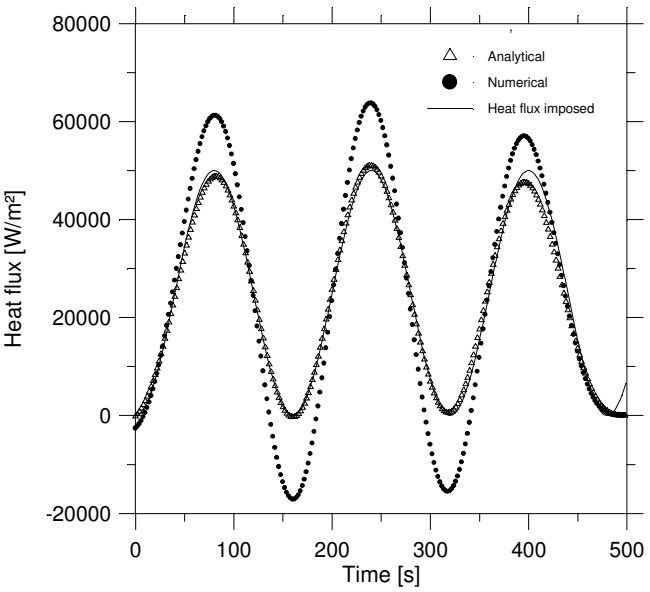

a)

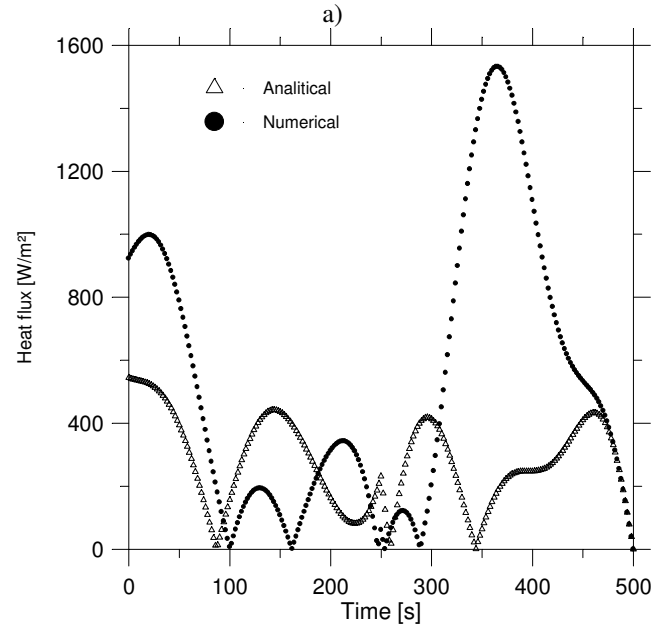

b)

Figure 10. Comparison between estimated and imposed sinusoidal heat flux: a) heat flux components; b) absolute residual error of heat flux components

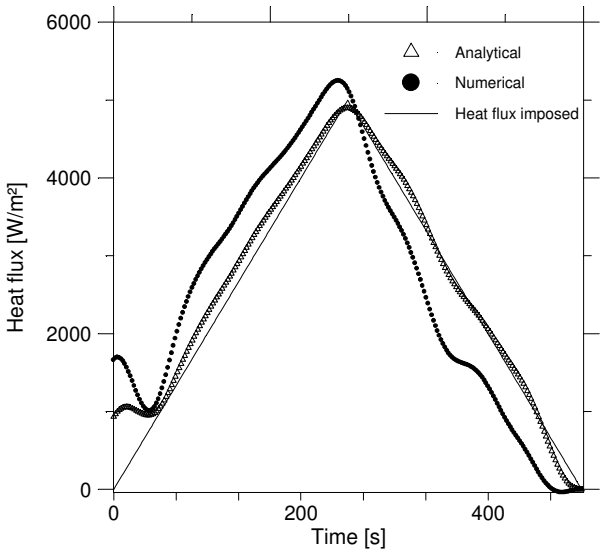

a)

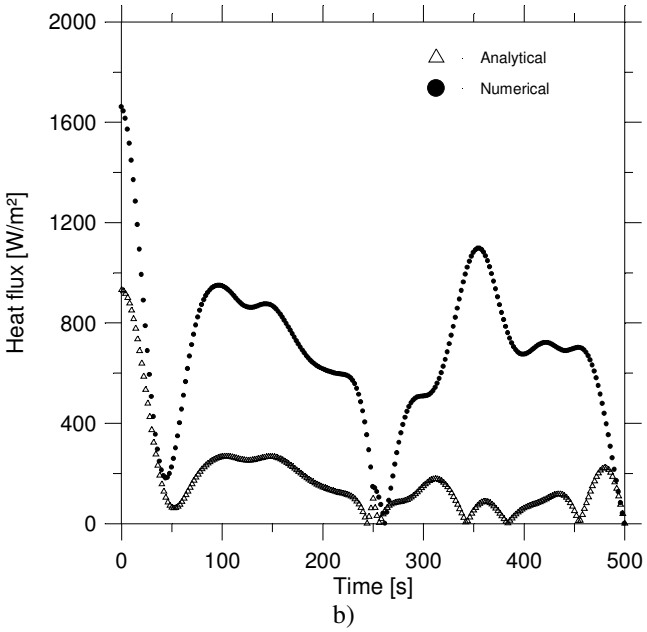

b)

Figure 11. Comparison between estimated and imposed triangular heat flux: a) heat flux components; b) absolute residual error of heat flux components

Heat flux estimation using simulated data from multiple sensors.

In order to verify the use of two or more thermocouples in the estimation results, Figure 12 presents a comparison between the estimation of heat flux using temperature simulated data using only one sensor and using heat transfer function equivalent for four sensors, nominated global heat transfer.

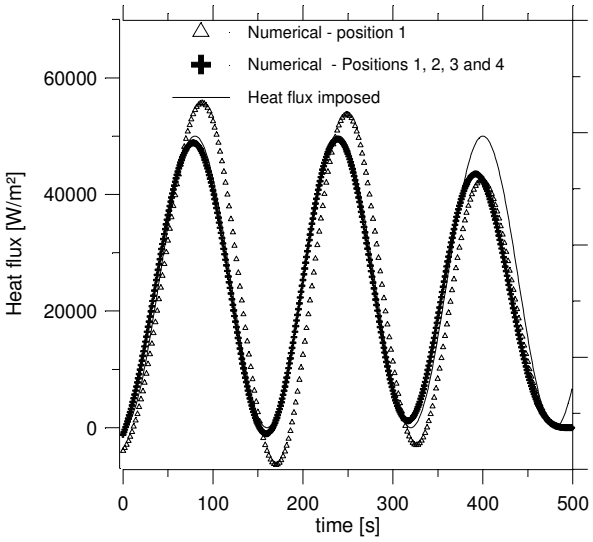

Figure 12. Comparison between estimated and imposed sinusoidal heat flux using G_H obtained numerically.

Data positions of simulated sensors used in the second improvement are presented in Table 1. The temperature data are used considering the global heat transfer function given by Eq.(29) for four temperatures. It can be observed that by using the new heat transfer function better results can be obtained.

Figure 13 presents a comparison of the heat flux estimation using the global heat transfer for the four positions with estimations using G_H obtained analytically. Figure 14 presents the residual error.

The good results for G_H shows the great flexibility of the technique to face a real problem where various thermocouples can be located in the sample. It can be noted that although both estimations are closer, the heat flux estimation using analytical functions present better results. This behavior is better observed in residual errors shown in Fig. 14.

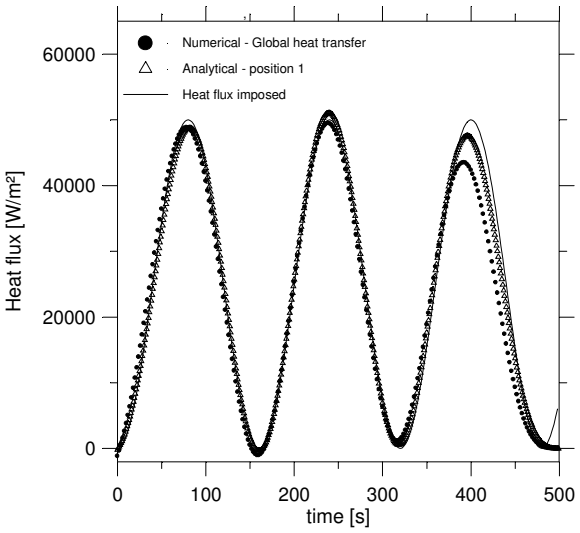

Figure 13. Comparison between estimated and imposed sinusoidal heat flux using G_H obtained numerically and analytically.

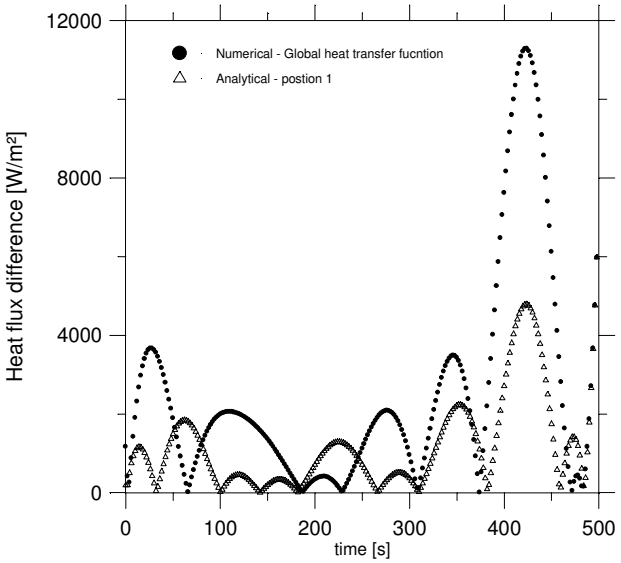

Figure 14. Comparison between estimated and imposed sinusoidal heat flux using single and global numerical heat transfer function.: a) heat flux components; b) heat flux residual error

Experimental test.

The new technique proposed here is now verified by estimating a heat flux imposed in a controlled experiment (Test 2). Figure 15 and Table 2 present the geometry and position of the thermocouple located in a AISI 304 sample.

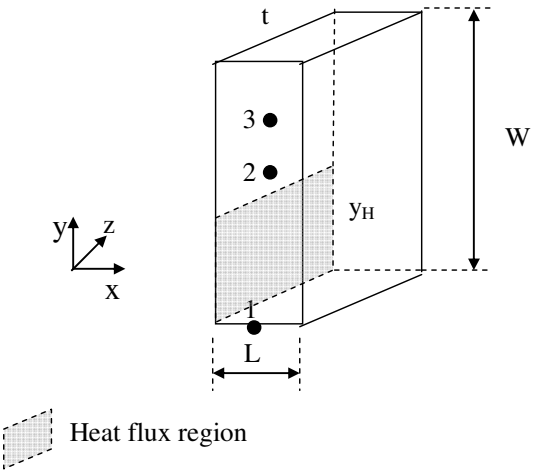

Figure 15. Experimental scheme for Test 2.

The AISI304 stainless steel sample used in the test has thickness of 6 mm and lateral dimensions of 50 x 138 mm. The sample initially in thermal equilibrium at T_0 is then submitted to a unidirectional and uniform heat flux. The heat flux is supplied by a 318 Ω electrical resistance heater, covered with silicone rubber, with lateral dimensions of 50 x 50 mm and thickness 0.3 mm. The temperatures are measured using surface thermocouples (type k). The signals of tension and current temperatures are acquired by a data acquisition system HP Series 75000 with voltmeter E1326B controlled by a personal computer.

Three thermocouples were brazed on the sample as shown in Figure 13. Their signals are shown in Fig. 16.

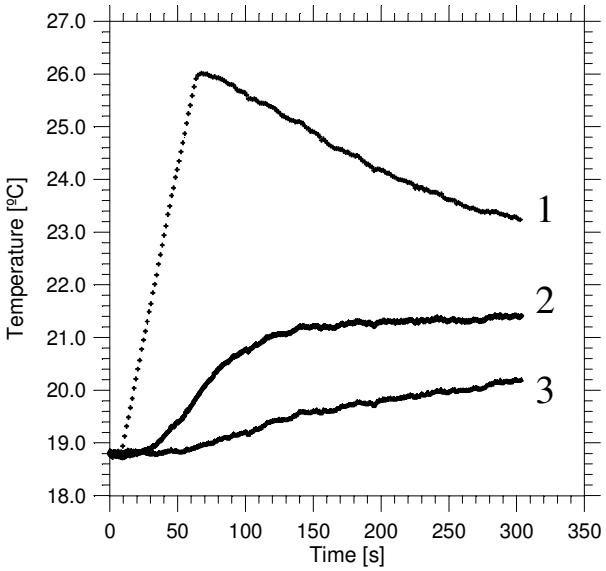

Figure 16. Experimental temperature evolution to thermocouple in position 1, 2 and 3 (Table 2).

Figure 17 shows the estimated heat flux using the technique described here and using the sequential function specification method described by Beck et al [3]. In order to compare the results, experimentally obtained temperatures were compared with estimated temperatures using the heat flux estimated by dynamic observer. This comparison is shown in Fig. 18. Residuals are presented in Fig. 19. The results show a difference less than 0.3 C that represents the uncertainty of thermocouple measurements.

To assure confidence in these results the total energy imposed by the electrical resistance over all time duration of experiment, 368 J, was compared with the total heat rate estimated. The energy estimated was calculated by integrating the heat flux component estimated over the time duration of the experiment. It was found that values were 379.5 J and 390 J for sequential method and dynamic observer, respectively. In this case the uncertainty was less than 3% for the technique proposed here. This result demonstrates the great power of the technique.

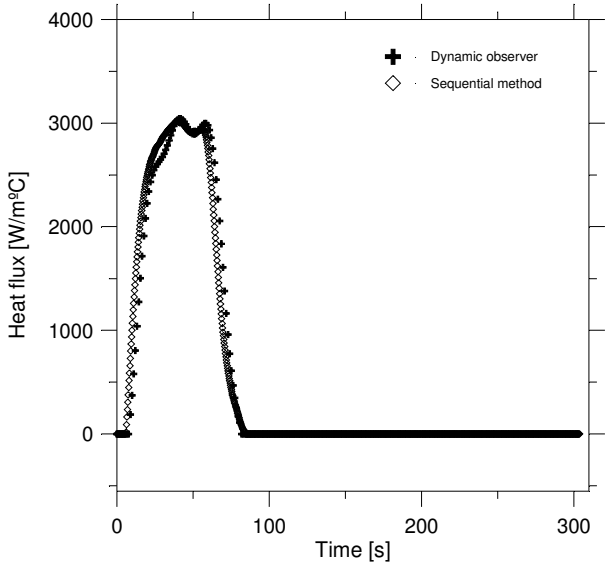

Figure 17. Heat flux estimation using sequential function specification and dynamic observer methods.

Table 2. Geometry and thermocouple position for Test 2

y_H=0.05m	L=0.006m	W=0.138 m	t=0.05m

position	x_i 10^{-3}[m]	y_i10^{-3}[m]	z_i10^{-3}[m]
1	11.5	62.5	25
2	0.0	62.5	25
3	10.0	86.0	25

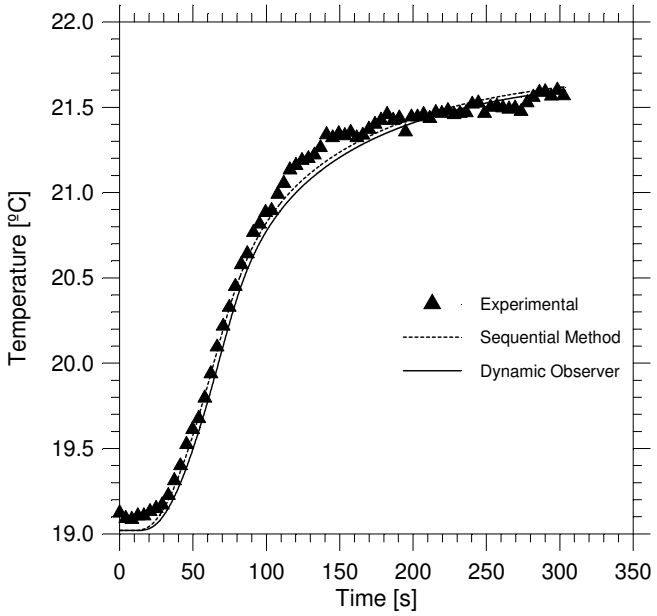

Figure 18. Comparison between the measured and estimated temperature using the heat flux estimated.

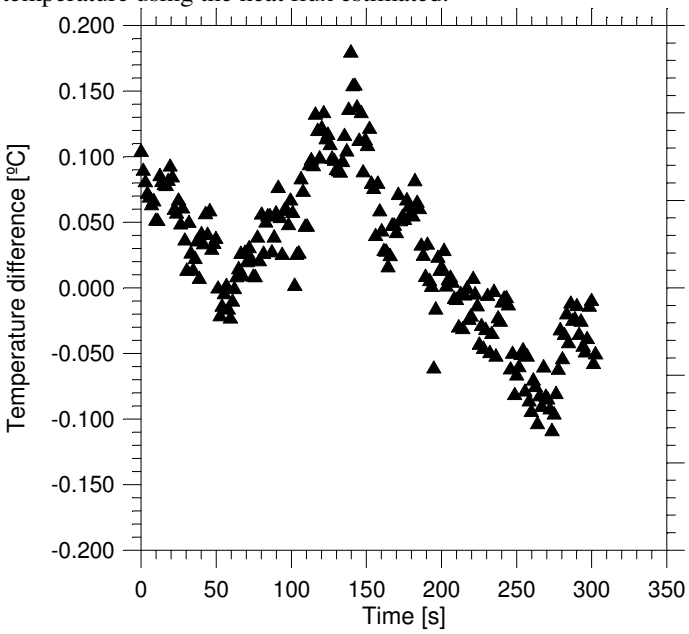

Figure 19. Comparison between the measured and estimated temperature using the heat flux estimated.

The great advantage of the dynamic observers technique is the easy and fast numerical implementation for any 1D, 2D or 3D model. The robustness and low computational cost and low error sensitivity gives this procedure a great potential in inverse techniques application. Obtaining 3D heat transfer functions is in progress.

CONCLUSION

The dynamic observer technique based on analytical Green function is presented here. The procedure used to obtain the analytical heat transfer gives more flexibility and robustness to the inverse procedure. The easiness of obtaining G_H for any position in the domain allows one to extend this technique to use more than one measured temperature.

ACKNOWLEDGMENTS

The authors thank to CAPES, Fapemig and CNPq.

REFERENCES

1. D. A. Murio, *The Molification Method and the Numerical Solution of Ill-Posed Problems*, John Wiley, New York, 1993

2. O. M. Alifanov, Solution of na Inverse Problem of Heat Conduction by Iterations Methods, *Journal of Engineering Physics, **10**. (1975)*

3. J. V. Beck, B. Blackwell, and C. R. St. Clair, *Inverse Heat Conduction, Ill-posed Problems*, Wiley Interscience Publication, New York, 1985

4. M. Raudensky, K. A. Woodbury, J. Kral, and T. Brezina, Genetic Algorithm in Solution of Inverse Heat Conduction Problems, *Numerical Heat Transfer. Part B, **28**, 293 (1995)*

5. C. V. Gonçalves, L. O. Vilarinho, A. Scotti, and G. Guimarães, G., Estimation of heat source and thermal efficiency in GTAW process by using inverse techniques, *Journal of Materials Processing Technology,(2006)*

6. S. R. Carvalho, S. M. M. Lima e Silva, A. Machado, G. Guimarães, G., Temperature Determination at the Chip-tool Interface Using an Inverse Thermal Model Considering the Tool and Tool Holder, *Journal of Materials Processing Technology, (2006)*

7. P. -C. Tuan, C-C. Ji, L.-W. Fong, and W.-T. Huang, An Input Estimation Approach To On-Line Two-Dimensional Inverse Heat Conduction Problems, *Numerical Heat Transfer, Part B, **29**,345 (1996)*.

8 J.W. Blum and W. Marquardt, An optimal solution to inverse heat conduction problems based on frequency-domain interpretation and observers", *Numerical Heat Transfer, Part B: Fundamentals, **32**, 453 (1997).*

9. Sousa, P. F. B., *Development of a technique Based on Green's Functions and Dynamic Observers to be Applied in Inverse Problems*, , Dissertation of Master's degree, Federal University of Uberlândia, Uberlândia, Mg. Brazil, 2006 (in Portuguese)

10. J. V., Beck, K. D. Cole, A. Haji-Sheik, B. Litkouhi,, *Heat Conduction Using Green's Function*, Hemisphere Publishing Corporation, USA, 1992, p. 523.

11. J. S. Bendat, A. G. Piersol, *Analysis and Measurement Procedures*, Wiley-Intersience, 2nd ed., USA, 1986, p. 566.